

## SCANNING ACOUSTIC MICROSCOPE FOR 3D IMAGING

Krzysztof DYNOWSKI, Jerzy LITNIEWSKI, Andrzej NOWICKI

Institute of Fundamental Technological Research  
Polish Academy of Sciences  
Świętokrzyska 21, 00-049 Warszawa, Poland  
e-mail: jlitn@ippt.gov.pl

*(received September 18, 2007; accepted April 11, 2008)*

A new Acoustic Microscope operating at the frequency up to 200 MHz and allowing for visualization of the internal structures of materials was developed. The system was built basing on the commercially available components and the self-designed acoustic lenses. The dedicated software was developed to control the process of 3D RF-data acquisition, processing and presenting in 2D cross-sections or 3D surface rendering mode. This article describes the technical principles of the constructed microscope and presents the reconstructed images of the designed test-probe and of the integrated circuit.

**Keywords:** Acoustic Microscopy, SAM, 3D imaging, rendering, subsurface imaging.

### 1. Introduction

Scanning Acoustic Microscopy (SAM) is a relatively new technique rapidly becoming established as a method for non-destructive evaluation (NDE) of engineering materials using high frequency ultrasound. Applications of acoustic microscopy make use of its ability to characterize material surface with high resolution. Taking an advantage of relatively low attenuation of the ultrasonic waves at very high frequency, acoustic microscope can penetrate materials that are opaque to the light [1, 2]. The following paper reveals the ability of SAM to visualize unseen internal tree dimensional structures.

The conventional SAM system operates as follows: The transmitting electronic system supplies electric short pulses to the piezoelectric transducer. The acoustic wave pulses generated by the transducer are transmitted along the lens rod to the spherical lens cavity. Then, the refracted and collimated waves propagate in the coupling fluid (usually water) toward the investigated specimen. The wave pulses back reflected from the surface or interfaces within the sample are collected by the lens and converted by the transducer into electrical signals. In order to obtain two-dimensional image the sample is scanned by the focused acoustic beam. The amplitude or phase of the reflected signals

from successive sampling points are stored and displayed on a monitor screen creating an image of acoustic and mechanical properties of the sample.

Two modes of visualization are usually used: C-scan and B-scan mode. In the C-scan mode, the collected reflected ultrasounds are time gated. Only the reflections from the focus are recorded and used for farther processing in order to measure amplitude or phase of the acoustic signal. The magnitude of one of these parameters is used to control the brightness of the image point. The acoustic lens with the transducer (often called the lens) is moved over the sample in raster pattern and the point by point two-dimensional image is build. Depending on the focus position, the C-scan mode allows to visualize the surface or an interior of the sample. The image reflects acoustic properties of the material at the plane perpendicular to the acoustic beam axis.

The B-scan mode is similar to the data acquisition used in ultrasonography. The signals reflected at each lens position are used to produce one line of the image. Therefore, only one-dimensional scanning is required to obtain two-dimensional image. This image corresponds to the cross-section of the sample, parallel to the acoustic beam axis.

The acoustic microscope presented in this paper combines C-scan and B-scan modes. The data collected during single XY scan allows to present transversal and horizontal cross-sections of the sample as well as real tree dimensional (3D) images of its interior.

SAM presented in this paper was originally built in Ultrasonic Department of IFTR (Fig. 1). The microscope was intended for subsurface imaging. The lateral resolution of SAM depends on the frequency of the acoustic waves, on the quality of the acoustic lens and on the properties of the material under investigations.

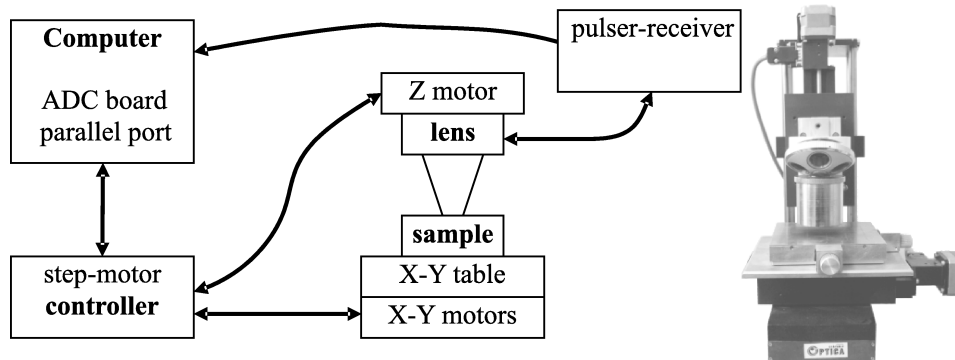


Fig. 1. Schematic diagram of the microscope.

Scanning microscope system modules:

- Mechanical scanner.
- Transmitter-receiver.
- Analog/Digital Converter board.
- Ultrasonic lens.
- Computer control and imaging software.

Mechanical scanner enables positioning of the ultrasonic lens over the investigated sample in the range of  $50 \text{ mm} \times 50 \text{ mm}$  with a high precision ( $2.5 \text{ }\mu\text{m}$  step). The commercial transmitting-receiving system (Panametrics, Inc., model 5900PR) was applied to excite the transducer at the frequency up to 200 MHz. The A/D converter board (Signatec, Inc., model PDA1000) was used for sampling and recording echo-signals originating in the sample. The system utilizes self-designed ultrasonic lenses that can operate in the frequency range 30 MHz – 200 MHz. The lenses were optimized for subsurface imaging taking into account geometrical aberration and refraction at the water-sample interface as well as internal spurious reflections within the lens rod [2].

The self-designed software is used to control the scanner motion and the sampling board operations. Also, the dedicated software was developed to collect the data and to transmit them into computer memory. In the next step the software processes the signal to remove internal lens reflections to increase signal-to-noise ratio, and to detect the amplitude, and finally reconstructs two or three-dimensional images using the vector graphics.

## 2. Data acquisition for 3D imaging

The sampling board of the microscope collects ultrasonic echoes – the object responses to the ultrasonic burst send into the sample. Figure 2a shows a typical sequence of R.F. signals recorded with the microscope (“oscilloscope” mode of the microscope). The presented signal consists of the transmitting electric signal, reflections within the sample and multiple ultrasonic reflections in coupling fluid and in the lens.

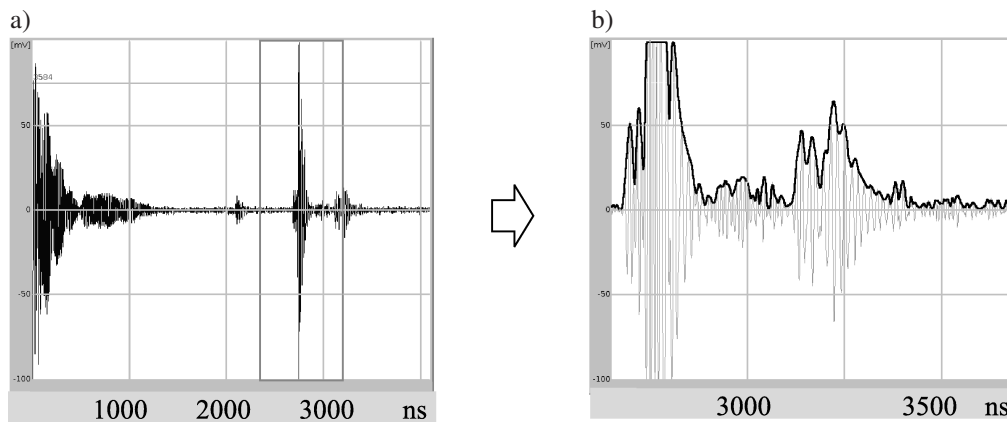


Fig. 2. The signal recorded from a microchip interior a) acoustic echoes and b) windowed part of amplified signal is shown together with the amplitude envelope, frequency 100 MHz.

To reduce the amount of data to be collected the region of interest (ROI) must be strictly defined. The size of ROI is given by the range of scanning ( $\Delta X \times \Delta Y$ ) and selected range of penetration depth inside the sample ( $\Delta Z$ ) (Fig. 2b). Assuming the wave

speed in the probe to be constant, the relationship between time ( $\Delta t$ ) and penetration depth ( $\Delta z$ ) is linear and can be described as

$$\Delta Z = \frac{1}{2} \Delta t \cdot c, \quad (1)$$

where  $c$  stands for the longitudinal wave velocity in the sample.

The proper selection of a limited-duration time period ( $\Delta t$ ) that contains echoes from the chosen internal structures and excludes the disturbing reflections, assures a good quality of images and reasonable time of data processing. In Fig. 2a a window is presented which is used to select a part of the signal that is next subjected to amplitude detection (Fig. 2b).

Three-dimensional image reconstruction of the selected region of a sample requires to store the RF responses from the object for each location of the microscope lens over the sample. Moving the lens along the  $X$ -axis the data for the B-scan image are obtained that corresponds to the transversal cross-section of the object. After recording the set of B-scans for successive positions of the lens along the  $Y$ -axis full three-dimensional data volume is collected (Fig. 3).

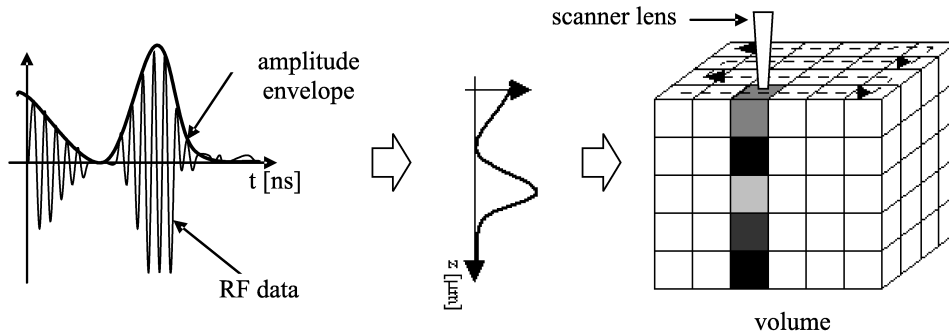


Fig. 3. The flow of the process creating the volumetric data set.

In Fig. 3 the process of the data acquisition is presented. For each of the recorded RF sequences the amplitude envelope is calculated. Next, the amplitude values are digitalized and linearly assigned to the gray-scale, and finally the volume (cuboid built of gray level values) is created. The elements of the volume correspond to the acoustic image of the sample but a lot of farther processing is necessary to visualize the internal structures in three-dimensional presentation.

### 3. Initial processing of data

The data stored in the volume must be processed to extract the position and the shape of the isolated physical structures hidden in acoustic noise. This processing is performed using self-developed software enabling 2D visualization of the sample cross-section (Fig. 4).

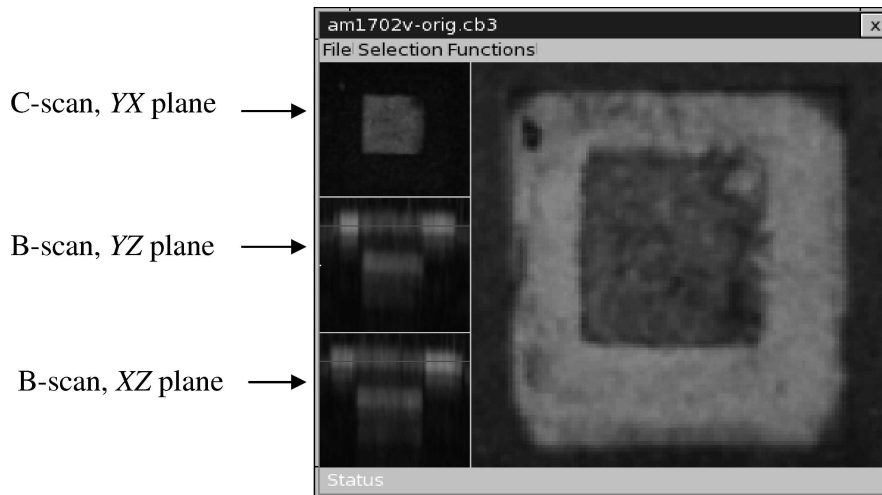


Fig. 4. Transversal cross-section of the microchip image.

The software contains several filtering procedures that enable selection of image points created by the signals reflected solely from internal structures. These procedures remove background and noise and are used to enhance intensity of the chosen points. Digital data processing are based on the filters: threshold, intensity, smooth, histogram equalization, boundary cutting (detailed description in Appendix).

The proper applying of the filtering functions results in “cleaning” of the volume data from disturbing components. These procedures operate correctly for small volume data. When the volume data are recorded for relatively thick sample the influence of the attenuation of ultrasonic waves and the influence of emitted pressure field structure results in the variation of the echoes’ intensity that is not related to imaging structures. Often, the compensation of these effects is not possible.

One of the solutions of this problem is the division of the *cube* into successive thin layers (perpendicular to *Z*-axis) and application of filters with different parameters for each layer. This solution works quite well when the objects inside the sample are the layered structures. If not, it is better to divide the cube into a set of *sub cubes* and to apply separate filtering for each of them.

The final step of 3D visualization is the transformation of the volume data (bitmap format) into 3D-vector graphics (ISO surface) that describes objects inside a volume sample.

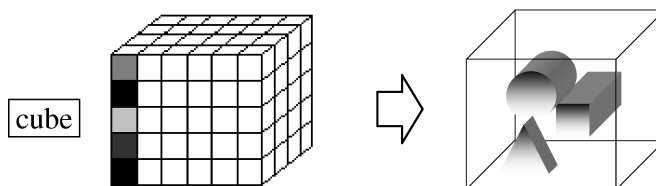


Fig. 5. Objects isolation – surface finding.

As a result of vectorization of the volume the collection of surfaces is produced (each surface is described by set of triangles – two vectors and vertex). The surface properties like: texture, color and light absorption can be assigned to each surface. These surfaces create objects in 3 dimensional space. Applying such effects like perspective, illumination, shading and obscuring farther objects by the nearer ones one can enhance the presentation of the objects. This significantly facilitates recognizing of objects by human eye.

To achieve vectorization we used VTK (Visualization Tool Kit) software from Kitware Inc., which is the open source software, designed for 3D graphics and image processing [6]. This system was extended with a *Volume Data Reader* module used for importing the data stored in the volume format and to transform them into a format used by VTK.

VTK software is based on the set of filters that operate in sequence on volume data and as the result they produce iso-surface – surface that represents points of constant value (gray-level). VTK implements a powerful algorithm of Compatible Triangulations [3]. This algorithm is based on several other algorithms, like ordered Delaunay triangulation, isocontouring adaptive grids, triangulation of unstructured grids, interval tetrahedrization and clipping.

The 3D triangulation is a general algorithm of spatial decomposition. Triangulation match edges and faces across spatial cell boundaries. The algorithm produces compatible triangulation on a cell-by-cell basis, using a modified Delaunay triangulation [5]. The algorithm is naturally parallel since it requires no neighborhood cell information, only a unique, global point numbering. The triangulation of grids must assure that the 1D triangulation of each cell edge is compatible with the corresponding edge of neighboring cell and the 2D triangulation of each cell face is compatible with the corresponding face of the neighbor.

#### 4. Results – 3 dimensional images

The imaging abilities of the microscope were tested using a custom-designed phantom. The phantom consisted of two copper wires (diameter of 0.25 mm and 0.5 mm) and a steel ball (diameter of 1 mm) embedded in the epoxy resin (longitudinal wave velocity = 2800 m/s). The microscope lens, optimized for imaging inside low velocity materials, was used in this test. The waves of 100 MHz frequency were focused inside the sample, approximately 1.0 mm under the surface. The sample was scanned and a volume of data was recorded and processed for imaging. The imaging volume size was equal to 7 mm × 7 mm × 2.4 mm (where 2.4 mm = 1/2 × 1800 ns × 2800 m/s). Two, selected projections of 3D image of this sample are presented in Fig. 6 and Fig. 7.

Also, the visualization of the interior of the material characterized with a high velocity was performed. To this end an integrated circuit (IC – AM1702) was used. The ceramic package-cover of the IC can be easily penetrated by 100 MHz ultrasounds. As the velocity in ceramic is much higher than in epoxy and consequently the wavelength is

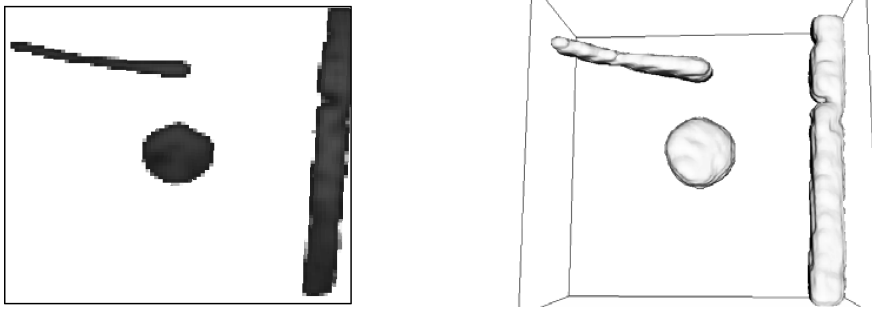


Fig. 6. 2D B-scan cross-section of the test sample a) and 3D projection of the same area b).

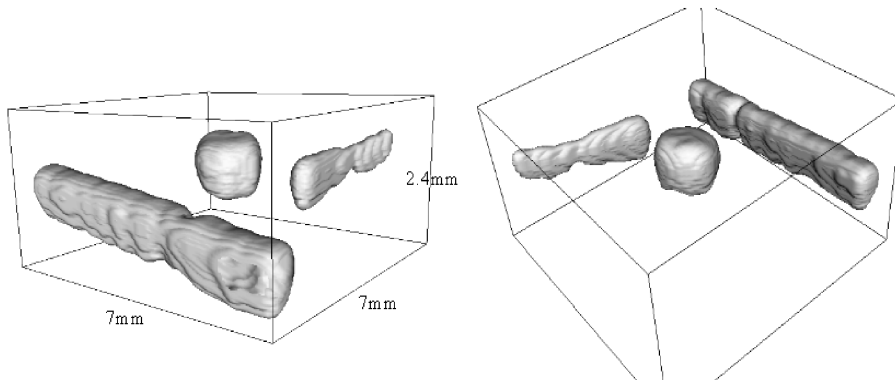


Fig. 7. Projections of 3D image of the test sample. Distortions of geometrical dimensions introduced due to the different velocity values in the objects and epoxy are clearly visible.

longer, the expected resolution of the image should be worse than for the testing sample. Also in this case the lens was optimized specifically for the subsurface imaging, this time in materials with the high velocity of ultrasounds (6000 m/s). The ultrasonic waves were focused inside the IC in the vicinity of the die plane. Figure 8 presents selected

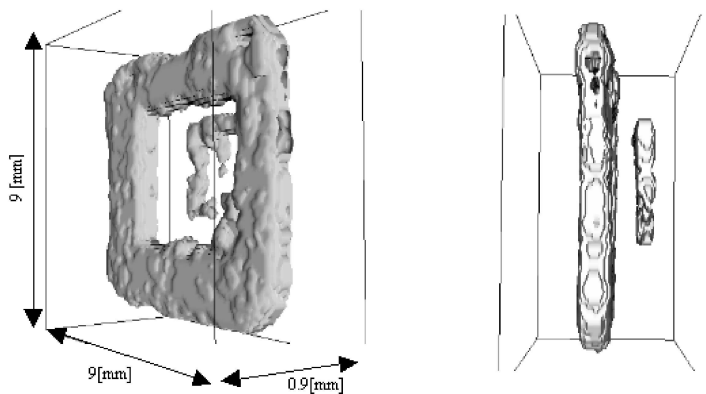


Fig. 8. Projections of 3D image of the IC sample.

projections of 3D IC-image built up basing on the data acquired by scanning the lens over the IC-sample. The imaging volume was equal to  $9 \text{ mm} \times 9 \text{ mm} \times 0.9 \text{ mm}$  (where  $0.9 \text{ mm} = 1/2 \times 300 \text{ ns} \times 6000 \text{ m/s}$ ).

## 5. Conclusions

The scanning acoustic microscope described in this paper can be used for imaging internal structures embedded in the material that is opaque for the light. The images are presented as 2D cross-sections of the sample or as 3D projections. The scene rendering GUI (graphical user interface) was used what allows for rotation of visualized objects and movements of observation point (camera). That significantly increases human perception and image recognition. The microscope can be used in material studies and microelectronics as well as for biological investigations.

The developed ultrasonic imaging system enables visualization of objects placed in the medium characterized by the low or high velocity of ultrasounds. The imaging resolution of the microscope, lateral and longitudinal, depends on material properties of the samples as these define the focused ultrasonic field properties and the length of the probing pulses. Also, as can be seen in the obtained images, the geometrical dimensions of the reconstructed structures depends on the ratio between the wave velocities in the material of the structures and surrounding medium. Only the 2D horizontal cross-section of the 3D image reflects the true relations between dimensions of visualized objects.

The microscope collects the RF data. Thus, the amplitude and the phase information can be exploit. This information will be used in the further study that will focus on the resolution enhancement and compensation of geometrical distortions in 3D images obtained with the microscope.

## Appendix

### • threshold value

This filtering allows to leave in the image only the points with gray-scale level exceeding defined threshold value. The points under this threshold are set to zero (black). The equation used for this filter is describe as:

$$\text{dst}[x, y, z] = \begin{cases} \text{src}[x, y, z], & \text{if } \text{src}[x, y, z] \geq \text{threshold}, \\ 0, & \text{if } \text{src}[x, y, z] < \text{threshold}, \end{cases} \quad \text{for every } x, y, z, \quad (2)$$

where  $\text{src}[x, y, z]$  and  $\text{dst}[x, y, z]$  denote respectively the gray-scale level of the source volume (src) and of the resulting destination volume (dst) in  $(x, y, z)$  point.

The histograms of the volume data are very useful in selecting parameters for the threshold value filter.

- **boundary cutting**

This procedure allows to select the part of the image of the investigated object. By cutting out this part, the amount of processed data is reduced, thus speeding up calculation time for all other functions.

$$\begin{aligned} \text{dst}[x - X_{\min}, y - Y_{\min}, z - Z_{\min}] &= \text{src}[x, y, z], \\ \text{for every } [x, y, z] &\in [X_{\min}, Y_{\min}, Z_{\min}], [X_{\max}, Y_{\max}, Z_{\max}], \end{aligned} \quad (3)$$

where  $X_{\min}$ ,  $Y_{\min}$ ,  $Z_{\min}$  and  $X_{\max}$ ,  $Y_{\max}$ ,  $Z_{\max}$  are minimum and maximum coordinates values that determine the selected part of data.

- **smoothing**

This filter enables to remove isolated peaks of intensity that often are met in the volume data. These peaks result from the statistical character of the received echo-signal (analogically to speckles in 2D ultrasonic images). The algorithm considers a set of points ( $3 \times 3 \times 3$  box) centered around the chosen point, removes the highest and the smallest value of point-intensity and then calculates the weighting average of remaining values and assigns the result to the considered chosen point. This algorithm is very helpful in preparing data for a surface (edge) finding procedure (in VTK – Visualization Tool Kit).

$$\text{dst}[x, y, z] = \frac{\sum_{[i,j,k]=[-N,-N,-N]}^{[N,N,N]} \text{src}[x+i, y+j, z+k]}{(2N+1)^3}, \quad \text{for every } [x, y, z], \quad (4)$$

where  $(2N+1)$  denotes smoothing box edge size.

- **intensity coefficient**

The procedure allows increasing or reducing image brightness using the following algorithm:

$$\text{dst}[x, y, z] = \begin{cases} \text{src}[x, y, z] \times \text{Coef}, & \text{if } \text{src}[x, y, z] \times \text{Coef} < L, \\ L, & \text{if } \text{src}[x, y, z] \times \text{Coef} \geq L, \end{cases} \quad \text{for every } x, y, z, \quad (5)$$

where Coef denotes intensity coefficient (Coef > 1 for the increase and  $0 < \text{Coef} < 1$  for the decrease of intensity) and  $L$  is total number of gray-scale levels.

- **histogram equalization**

The procedure increases contrast enhancement using the following algorithm:

First the probability ( $p_i$ ) of an occurrence of a pixel of level  $i$  in the volume is calculated.

$$p_i = \frac{n_i}{n}, \quad \text{for } i \in 0, 1, 2 \dots L-1, \quad (6)$$

where  $L$  is total number of gray-scale levels,  $n_i$  the number of occurrences of gray level  $i$  and  $n$  total number of pixels, and  $p$  is in fact the image's histogram, normalized to domain 0..1.

Next the cumulative distribution function –  $C$  (also known as accumulated normalized histogram) is determined:

$$C_i = \sum_{j=0}^i p_j, \quad \text{for } i \in 0, 1, 2, \dots, L-1. \quad (7)$$

The  $C_i$  maps the levels into the domain of 0..1. In the last step the program maps the gray-scale values back to their original domain using the following simple transformation:

$$\text{dst}[x, y, z] = (L-1) * C_{\text{src}[x,y,z]}, \quad \text{for every } x, y, z. \quad (8)$$

### Acknowledgments

This study was supported by Ministry of Science and Higher Education, Poland (grant no. 3 T11E 011 30).

### References

- [1] BRIGGS A., *Advances in acoustic microscopy*, Vol. I, II of Plenum Press, New York 1995, 1996.
- [2] LITNIEWSKI J., *Subsurface imaging of samples by SAM*, Archives of Acoustics, 19, 4, 487–493 (1994).
- [3] NIKOLAIDIS N., PITAS I., *3-D Image Processing Algorithms*, Wiley-Interscience Pub., New York 2001.
- [4] SCHROEDER W.J., GEVECI B., MALATERRE M., *Compatible triangulations of spatial decompositions*, [in:] Proceedings of Visualization 2004, pp. 211–218, Austin, USA IEEE Press, October, 2004.
- [5] DELAUNAY B., Sur la sphère vide, *Izvestia Akademii Nauk SSSR*, Otdelenie Matematicheskikh i Estestvennykh Nauk, 7, 793–800 (1934).
- [6] SCHROEDER W., MARTIN K., LORENSEN B., *Visualization Toolkit an object-oriented approach to 3D graphics*, 4th Edition, Kitware Inc. 1997.